

Nonthermal X-radiation of SNR RX J1713.7–3946: The Relations to a Nearby Molecular Cloud

Y. Uchiyama^{*}, F. A. Aharonian[†], T. Takahashi^{**‡}, J. S. Hiraga^{**},
Y. Moriguchi[§] and Y. Fukui[§]

^{*}*Yale Center for Astronomy and Astrophysics, Yale University, P.O. Box 208121,
New Haven, CT 06520-8121, USA*

[†]*Max-Planck-Institut für Kernphysik, Postfach 103980, D-69029 Heidelberg, Germany*

^{**}*Institute of Space and Astronautical Science, JAXA, Sagami-hara, Kanagawa 229-8510, Japan*

[‡]*Department of Physics, University of Tokyo, Bunkyo-ku, Tokyo 113-0033, Japan*

[§]*Department of Astrophysics, Nagoya University, Furo-cho, Chikusa-ku, Nagoya 464-8602, Japan*

Abstract. The recent X-ray and CO observations of RX J1713.7–3946 show that a significant fraction of the nonthermal X-ray emission of this unique supernova remnant associates, in one way or another, with a molecular cloud interacting with the west part of the shell. This adds a new puzzle in the origin of X-ray emission which cannot be easily explained within the standard model in accordance of which X-rays are result of synchrotron radiation of multi-TeV electrons accelerated by strong shock waves. We explore an alternative origin of the X-ray emission assuming that it is produced by secondary e^\pm resulting from high energy hadronic interactions in the molecular gas. Such a scenario could explain in a quite natural way the apparent correlation between the X-ray and CO morphologies. However, the TeV γ -ray emission recently reported by H.E.S.S. significantly constrains the parameter space of this model. Namely, this mechanism cannot reproduce the bulk of the observed X-ray flux unless one postulates existence of a *PeV cosmic-ray component* penetrating with an unusually hard spectrum into the dense cloud.

SNR RX J1713.7–3946: BRIEF SUMMARY

The SNR RX J1713.7–3946 exhibits remarkable nonthermal X-ray emission, with the largest total energy flux of $\simeq 5 \times 10^{-10}$ erg cm⁻² s⁻¹ (2–10 keV) amongst the shell-type SNRs. The diffuse X-ray emission, presumably of synchrotron origin, is distributed over the entire SNR. It is characterized by a power-law spectrum with an average photon index $\Gamma \simeq 2.3$ [1, 2].

The observations of this source with *Chandra* [3, 4] revealed that the bright north-western (NW) rim is comprised of a complex network of filaments and hotspots embedded in diffuse emission. The X-ray spectra of these sub-components in the NW rim are well fitted by a power law with variation of the photon indices within $\Gamma \simeq 2.1$ – 2.5 [3]. Recently, similar spatial and spectral characteristics have been found in the south-western (SW) rim in the *XMM-Newton* data [5, 6]. The applicability of the standard shock-acceleration (more specifically, diffusive shock acceleration) scenario to the synchrotron X-ray emission in RX J1713.7–3946 has been disputed based on the lack of indication of the expected (within the framework of this model) cutoff energy below 10

keV [3].

Originally it has been claimed that the molecular clouds found at a distance of 6 kpc are associated with this SNR [2]. Therefore the distance to the SNR has been widely adopted as 6 kpc. However, the recent CO observations made with the sensitive *NANTEN* telescope have revealed a strong indication of interaction of a molecular cloud located at a distance of 1 kpc with RX J1713.7–3946 [7]. This finding is further strengthened by an elaborate comparison between the X-ray and molecular emissions presented below and by the X-ray absorption features [8]. The atomic and molecular hydrogen column density toward the line-of-sight of the X-ray nebula becomes comparable to X-ray absorbing column density at $\simeq 1$ kpc [9], which also supports the association with the nearby molecular cloud. The $\simeq 1$ kpc distance to the supernova remnant makes plausible its association with the guest star A.D. 393 [10] (the remnant age of $t_{\text{age}} \simeq 1600$ yr).

The CANGAROO collaboration reported the detection of TeV γ -ray emission from the direction of the NW rim [11, 12]. The spectrum was claimed to be quite steep with a power-law photon index $\Gamma = 2.8 \pm 0.2$ (0.4–8 TeV). It was argued that the steep spectrum is inconsistent with the inverse Compton model, but could be explained by π^0 -decay γ -rays [12]. Most recently, the H.E.S.S. collaboration announced detection of TeV γ -rays *distributed over the entire X-ray nebula* with a hard power-law spectrum $\Gamma = 2.2 \pm 0.1$ (1–10 TeV) and flux 3.5×10^{-11} erg cm $^{-2}$ s $^{-1}$ [13]. The fascinating γ -ray image detected by H.E.S.S. appears to be generally similar to (although not exactly same as) the X-ray image.

In this paper we compare the spatial structures of the nonthermal X-ray nebula RX J1713.7–3946 with the CO image of the interacting molecular cloud, and briefly discuss the origin of X-radiation which seems to be quite different from synchrotron X-ray emissions of other young shell-type SNRs [14], and explore the capability of secondary e^\pm , generated through hadronic collisions in the cloud, to explain the X-ray nebula. Details will be presented elsewhere [8].

RX J1713.7–3946: COMPARISON BETWEEN NONTHERMAL X-RAY AND CO EMISSIONS

In Fig. 1, the overall X-ray nebula is compared with the *NANTEN* CO distribution of the nearby interacting molecular cloud. The X-ray nebula shapes a large parallelogram ($60' \times 70'$), with enhanced brightness in the northwest and southwest parts, which we refer as “NW rim” and “SW rim”, respectively. These rims with an apparent width $\sim 10'$ have been extensively examined in Refs. [3, 4, 5, 6]. The bright NW and SW rims appear to be buried in the molecular cloud. Four CO peaks (A, B, C, and D) are all located in the western part of the nebula. A direct correlation between the X-ray and CO emissions can be seen for peak C, from which the broad-line component of CO emission, a good indicator of SNR interactions [15], has been detected [7]. This morphological comparison suggests that the dense molecular gas somehow plays a crucial role for the formation of the bright nonthermal X-ray rims.

A close-up X-ray image of the SW portion, where the major CO peaks are located, is displayed in Fig. 2a together with the CO($J=1-0$) intensity map. The *XMM-Newton*

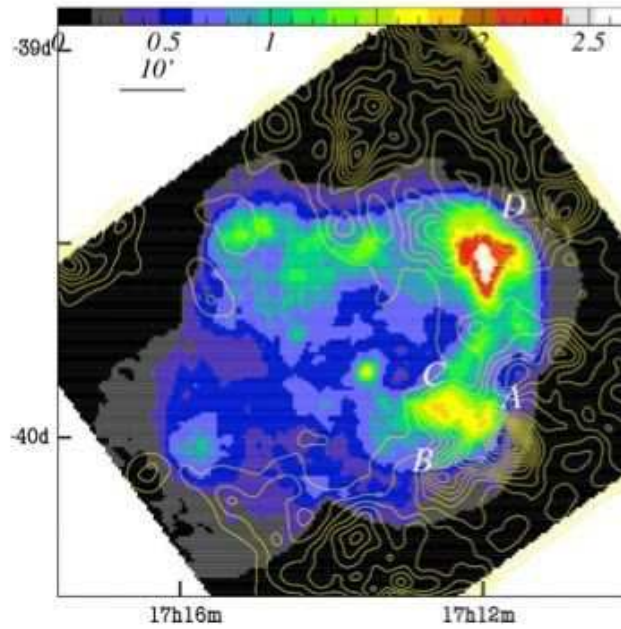


FIGURE 1. ASCA X-ray image (1–5 keV) of RX J1713.7–3946 overlaid with CO($J=1-0$) map (contours) in the velocity range from -11 to -3 km s^{-1} . The X-ray intensity scale is $\text{counts ks}^{-1} \text{pixel}^{-1}$ with a pixel size of $\approx 0.5'$. The CO contours are every 2 K km s^{-1} in the range of $2-30$ K km s^{-1} . North is up and east is to the left.

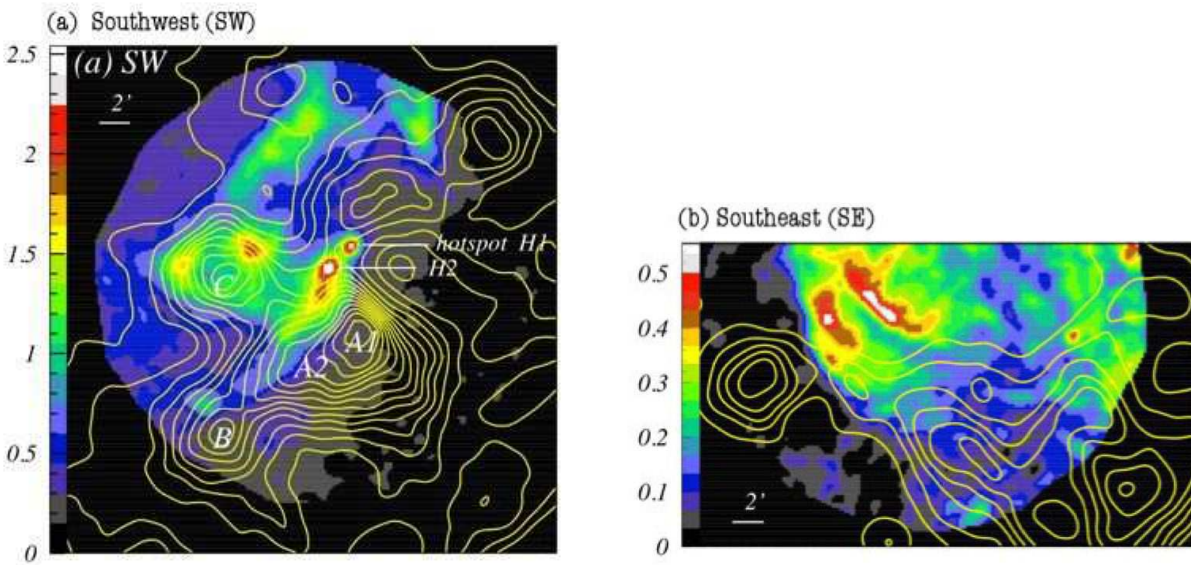


FIGURE 2. XMM MOS images (0.6–5 keV) accumulated in $10'' \times 10''$ pixels with the same CO map used in Fig. 1 overlaid. The X-ray intensity scale is $\text{counts ks}^{-1} \text{pixel}^{-1}$. North is up and east is to the left. **a)** For the SW part. The CO contours are every 2 K km s^{-1} from 2 to 30 K km s^{-1} . **b)** For the SE part. The CO contours are from 1 to 8 K km s^{-1} with an interval of 1 K km s^{-1} .

image demonstrates that the CO peak C has excellent spatial match with the nonthermal X-ray emission. Through spectral analysis, we found that the X-ray emission from peak C experiences additional soft X-ray absorption ($\Delta N_{\text{H}} \simeq 2 \times 10^{21} \text{ cm}^{-2}$), confirming the association with the CO peak. Also we found another bright X-ray feature that correlates well with the CO clumps, lying at the northeastern edge (a steep gradient of the CO line intensity) of peak A (A1+A2). The X-ray spectra of these bright features have a photon index $\Gamma \simeq 2.3$, quite typical for the west part of the rim.

In Fig. 2b, we also present the X-ray image of the southeastern (SE) sub-field, where the X-ray intensity is very low. The faint diffuse X-ray emission seems to associate with the molecular gas in the SE field. Interestingly, while in the SW rim the *brightest* X-ray features emanate from the molecular cloud, in the SE part the faintest appear to originate from the cloud. The X-ray spectrum extending up to at least 5 keV suggests nonthermal origin, although the faintness of the X-ray emission from this region does not unfortunately allow a detailed spectral study.

The results presented in Figs. 2a,b imply that the nonthermal X-ray emission emanates directly from dense molecular gas (though it cannot be excluded that a part of the emission originates in hot tenuous plasma). Usual synchrotron interpretation for the X-ray emission requires presence of multi-TeV electrons in the molecular cloud. Acceleration of multi-TeV electrons *inside* the molecular cloud, however, is unlikely with conventional shock-acceleration models. Slow shock waves propagating inside the dense cloud ($v \ll 1000 \text{ km s}^{-1}$) are not fast enough to accelerate electrons to very high energies; the diffusive shock acceleration time scales as $t_{\text{acc}} \propto v^{-2}$, where v is the shock velocity.

Yet *external acceleration* scenarios also involve some difficulties. Suppose, for example, that the fast supernova shock expanding into the stellar wind bubble accelerates multi-TeV electrons and injects them into the molecular cloud resulting in synchrotron X-ray emission. The ultra-relativistic electrons are subject of severe synchrotron losses as passing through the magnetized cloud, with synchrotron cooling time $t_{\text{syn}} \simeq 240 \text{ yr}$ for a moderate magnetic field of $B = 30 \mu\text{G}$. Unless the X-ray nebula is extremely young ($t_{\text{age}} < t_{\text{syn}}$), one should observe *aging* effects of synchrotron-emitting electrons. Nevertheless, we measured *hard* synchrotron X-ray spectra ($\Gamma \simeq 2.3$) throughout the NW and SW rims, which seems to argue against external origins of the X-ray emitting electrons.

The power-law spectra of synchrotron X-rays measured in this nebula suggest synchrotron cutoffs located at energies beyond $\varepsilon_0 \gtrsim 10 \text{ keV}$ [3]. On the other hand, within the standard framework of diffusive shock acceleration, the synchrotron cutoff should be located well below 10 keV.

Therefore it is important to explore other possible (alternative) models for interpretation of the spectral and spatial features of the observed nonthermal X-ray emission. Below we discuss the capability of a hadronic model to explain a non-negligible fraction of X-rays by synchrotron emission of electrons from decays of secondary π^{\pm} mesons produced in hadronic interactions.

SECONDARY-ELECTRON SYNCHROTRON X-RADIATION

Interactions of accelerated protons with the ambient gas lead to the production of π -mesons with comparable fractions of the energy of primary protons transferred to the final products of π -meson decays— γ -rays, electrons and neutrinos. While γ -rays and neutrinos freely escape their production regions and can be observed directly, the secondary electrons lose their energy through synchrotron radiation and inverse Compton scattering. In presence of sufficiently large magnetic field, e.g. close to $100 \mu\text{G}$ or more, which is needed for acceleration of protons to PeV energies, the bulk of the electron energy is released in the form of hard X-rays. The production of X-rays by secondary electrons is an attractive possibility which to a large extent is free of the problems associated with the synchrotron radiation by *directly accelerated electrons*. In particular, this model allows diffuse synchrotron X-ray emission throughout the remnant (because the protons can propagate without significant losses), as well as allows extension of X-ray spectra well above 10 keV.

One may expect that *directly accelerated* electrons are dominant contributors to synchrotron X-ray emission, rather than the secondary electrons. Actually, indeed the primary synchrotron X-radiation can exceed the contribution by the secondary electrons by more than an order of magnitude for shell-type SNRs with low ambient density, e.g. $n \sim 1 \text{ cm}^{-3}$ and a proton-to-electron ratio ~ 100 . However, since the cease of particle injection quickly results in a dramatic drop of the X-ray flux by primary electrons on a timescale $t_{\text{syn}} \approx 100 \text{ yr}$, while the X-ray flux by secondaries remains unchanged on much longer timescale $\tau_{\text{pp}} \gtrsim 10^5 \text{ yr}$, in the case of a “dead” accelerator (e.g. due to the crash of the shell with a dense cloud) we may expect X-radiation only from secondary electrons. Moreover, in dense environments, like molecular clouds interacting with the SNR shell, the synchrotron X-radiation may dominate even in the case of an active accelerator.

Finally, the long-lived ultrarelativistic protons can propagate throughout the dense gas generating secondary e^\pm via the production and subsequent decay of charged pions. Unlike directly accelerated electrons which are expected to be concentrated in the proximity of their acceleration sites, the secondary electrons can be easily distributed over larger volume, resulting in extended synchrotron radiation as observed.

In Fig. 3, we show a characteristic example of broad-band SEDs of nonthermal radiation resulting from pp interactions, assuming that protons are injected into the production region with a (number) spectrum $Q \propto E^{-1.9} e^{-E/E_0}$. It is seen that for the sufficiently high cutoff energy in the spectrum of protons ($E_0 \geq 1 \text{ PeV}$), the secondary synchrotron X-ray flux becomes comparable to that of π^0 -decay γ -rays. Since the π^0 -decay γ -rays are tightly coupled in such a way with the synchrotron radiation of secondary electrons, the TeV γ -rays flux detected by H.E.S.S. [13] constrains the level of the X-ray flux contributed by secondary electrons. Note that the π^0 components shown in Fig. 3 correspond to the H.E.S.S. flux from the NW part. Since the accompanying X-ray flux by secondary-electrons falls well below (by an order of magnitude) the observed X-ray flux (at several mCrab level), one may conclude that the contribution by secondary electrons cannot exceed 10 percent of the observed X-ray flux.

However, the relative contribution of X-rays can be significantly increased without violating the H.E.S.S. flux if one assumes very hard proton spectrum, e.g. $Q \propto E^{-1.5}$,

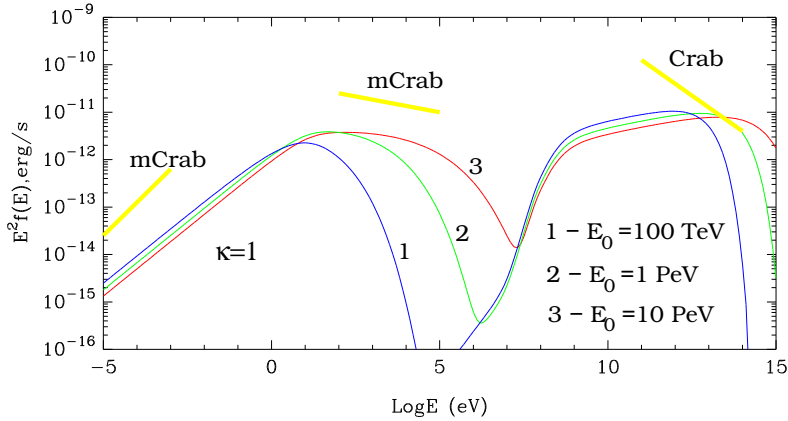


FIGURE 3. The broadband SEDs of radiation (secondary e^\pm synchrotron and π^0 -decay gamma-rays) initiated by p - p interactions. It is assumed that protons are injected continuously into a dense region with linear size $R = 1$ pc, gas density $n = 100 \text{ cm}^{-3}$, and magnetic field $B = 100 \mu\text{G}$. The injection spectrum of protons is a power law with spectral index $s = 1.9$ and exponential cutoff $E_0 = 0.1$ PeV, 1 PeV, and 10 PeV. The source age 1000 yr. The proton injection power $L_p = 3 \times 10^{37} \text{ erg s}^{-1}$ (total injected energy $W_p \simeq 1 \times 10^{48} \text{ erg}$). The escape time of protons in the source is set assuming Bohm diffusion.

extending to PeV energies. It should be noted that such a hard component of cosmic rays is not excluded by the nonlinear shock acceleration theory [16]. Also, very hard proton spectra can be expected due to propagation effect. For example, it is possible, at least in principle, that due to very slow diffusion only ≥ 1 PeV protons can arrive, for the limited age of the accelerator, at the dense regions of the clouds. In this case formally we can expect an arbitrary hard proton spectrum which in the regions of enhanced density may initiate secondary radiation with unusual SEDs—with distinct peaks at the hard X-ray and ultrahigh energy γ -ray domains.

REFERENCES

1. Koyama, K., Kinugasa, K., Matsuzaki, K., et al. *PASJ*, **49**, L7–L11 (1997).
2. Slane, P., Gaensler, B. M., Dame, T. M., et al. *ApJ*, **525**, 357–367 (1999).
3. Uchiyama, Y., Aharonian, F. A., and Takahashi, T., *A&A*, **400**, 567–574 (2003).
4. Lazendic, J. S., Slane, P. O., Gaensler, B. M., et al. *ApJ*, **602**, 271–285 (2004).
5. Cassam-Chenai, G., Decourchelle, A., and Ballet, J., *A&A* (2004), in press.
6. Hiraga, J. S., Uchiyama, Y., Takahashi, T., and Aharonian, F. A., *A&A* (2004), in press.
7. Fukui, Y., Moriguchi, Y., Tamura, K., et al. *PASJ*, **55**, L61–L64 (2003).
8. Uchiyama, Y., Aharonian, F. A., Derishev, E., et al. (2004), in prep.
9. Koo, B.-C., Kang, J., and McClure-Griffiths, N., “HI Study of Southern Galactic Supernova Remnants,” in *IAU Symposium*, 2004, p. 85.
10. Wang, Z. R., Qu, Q.-Y., and Chen, Y., *A&A*, **318**, L59–L61 (1997).
11. Muraishi, H., Tanimori, T., Yanagita, S., et al. *A&A*, **354**, L57–L61 (2000).
12. Enomoto, R., Tanimori, T., Naito, T., et al. *Nature*, **416**, 823–826 (2002).
13. Berge, D. (H.E.S.S. collaboration), *these proceedings* (2004).
14. Vink, J., *these proceedings* (2004).
15. White, G. J., Rainey, R., Hayashi, S. S., and Kaifu, N., *A&A*, **173**, 337–346 (1987).
16. Malkov, M. A., and O’C Drury, L., *Reports of Progress in Physics*, **64**, 429–481 (2001).